BOLETIN DE LA SOCIEDAD ESPAÑOLA DE
Cerámica y Vidrio
A R T I C U L O

Electrical conductivity of Yttria Stabilized Zirconia (YSC) doped with transition metals

R. M. SLILATY, F. M . B. MARQUES
Ceramics and Glass Engineering Department, University of Aveiro.
3810 Aveiro, Portugal

The effects of small additions of transition metal dopants (Fe, Mn and Cr) on the structure and conductivity of yttria stabilized zirconia (YSZ) have been investigated by XRD, SEM and electrical measurements. YSZ was doped with 1, 3, and 5 % of dopant cations using a mixed oxide technique. Impedance spectroscopy techniques illustrate that Mn doped compositions showed the most dramatic changes, and Cr doped compositions most closely approximated pure YSZ. Constant frequency (10 kHz) conductivity measurements were performed as a function of oxygen partial pressure in the range 800-1100 °C. At high temperature, for zirconia based systems, the cell impedance at this frequency is usually representative of the bulk material behavior. However, the presence of the transition metal dopants resulted in a shift of this frequency response, inducing errors when calculating the conductivity from these constant frequency measurements. In fact, the ac conductivity was found constant for oxygen partial pressures from 10^{-20}-10^{5} Pa, as confirmed by impedance spectroscopy measurements taken during the oxidation-reduction cycle. This suggests that these small dopant concentrations do not significantly influence the electronic conductivity of YSZ.

Keywords: Zircona, Transition metal, Impedance spectroscopy

Conductividad eléctrica de Circona Estabilizada con Itria (YSZ) dopada con óxidos de metales de transición

Se ha investigado en este trabajo, mediante las técnicas de DRX, MEB y medidas eléctricas, el efecto de pequeñas adiciones de dopantes de metales de transición (Fe, Mn y Cr), sobre la estructura y conductividad de la circona estabilizada con itria. Las muestras de YSZ fueron dopadas com 1, 3 y 5% (molar) de cationes dopantes mediante la técnica de mezcla mecánica de óxidos. Las técnicas de espectroscopia de impedancia indican que las composiciones dopadas con Mn muestran los cambios más dramáticos, mientras que las que fueron dopadas con Cr son las que más se aproximan al comportamiento de la YSZ pura. La conductividad a frequencia constante (10 kHz) se llevó a cabo en función de la presion parcial de oxigeno en el intervalo de temperatura entre 800-1100°C. A temperaturas altas, para los sistemas basados en circona, la impedancia de la célula electroquímica a dicha frequencia es normalmente representativa del comportamiento del interior de grano. Sin embargo, la presencia de los dopantes de metales de transición provoca um cambio en la respuesta del material a dicha frecuencia, lo que induce a cometer errores al calcular la conductividad a partir de las medidas a frecuencia constante. De hecho, la conductividad en corriente alterna (ac) fué constante en el intervalo de presiones parciales de oxigeno desde 10^{-20} a 10^{5} Pa, resultado confirmado por las medidas de espectroscopia de impedancia compleja, que fueron tomadas durante los ciclos de oxidación-reducción. Esto sugiere que estas pequeñas concentraciones de dopante no influyen significativamente en la conductividad electrónica de la YSZ.

Palabras clave: Circona, metal de transición, espectroscopia de impedancia

1. INTRODUCTION

Zirconia-based electrolyte systems are of widespread use in high temperature oxygen sensors, solid oxide fuel cells (SOFCs) and steam electrolysers (SE). Zirconia systems are preferred over others (e.g. ceria, hafnia, bismuth oxide) due to a unique combination of good electrical, mechanical, and chemical properties. The ionic conductivity of zirconia electrolytes is relatively high, and ionic domains are large enough for most envisaged applications. Good chemical stability exists within a large range of working conditions, including severely reducing atmospheres. Additionally, on changing the dopant types and levels (Sc_2O_3, Y_2O_3, CaO, etc.) improved performance can be obtained with respect to one or more of the above mentioned criteria (1).

The effect of different dopants on the properties of zirconia materials has been extensively studied in attempts to improve electrical properties while preserving the remaining properties. Yttria stabilized zirconia (YSZ) is one of the most representative examples of zirconia-based electrolytes. Previous studies have focussed upon doping YSZ with mixed valence cations, so as to obtain ionic + electronic conductivity under reducing conditions. CeO_2 and TiO_2 as dopants were indeed found effective in promoting mixed conductivity under reducing conditions. It is commonly accepted that the enhancement of the electronic conductivity in these materials is the result of the formation of oxygen vacancies and electronic defects at higher oxygen activities than expected for undoped YSZ. This change in YSZ redox behavior is the result of the dopant addition, and follows the redox behavior of the single oxide quite closely (2-6). The effect of transition metal oxides like Fe, Mn, Cr, etc., was also studied,

but less information is available on these systems, and at times conflicting evidence is found due to different processing routes. A general observation is that the conductivity of YSZ drops with such additions and in some cases an enhancement in electronic conductivity is also reported (7-11).

The development of SOFCs, devices whose lifetime is expected to be on the order of thousands of hours, further suggests a careful evaluation on the role of transition metal cations on the properties of YSZ. These metals might be present in different components of the SOFC system (e.g. cathode and interconnection material in the Westinghouse concept (12), cathode and metallic plate in the Siemens concept (13)). Long term contact between the cell components may allow for diffusion of cations into the electrolyte, and therefore, the impact of the presence of these impurities on cell performance merits attention. Recent studies have also reported that the cathodic overpotential of transition metal doped YSZ was reduced compared to YSZ alone (14). Thus, the present work aims at further determining the effects of transition metals on YSZ performance.

2. EXPERIMENTAL PROCEDURE

A commercial YSZ (8 mol % Y_2O_3 doped ZrO_2) powder from Tosoh was chosen as the base material. Three transition metal dopants were studied: Fe, Mn, and Cr. Doping levels were 1, 3, or 5 % of the respective cation concentration. Compositions will thus be identified using the nomenclature xMYSZ, where x corresponds to the doping level and M the transition metal (M=Fe, Cr or Mn; e.g. 1FeYSZ, 5MnYSZ).

YSZ powder was wet-milled in ethanol (96 v/o) with an oxide or carbonate powder of the dopant element. All mixtures were then dried, uniaxially pressed and sintered for 2 h to obtain dense samples of approximately 2 mm thickness. Compositions containing Fe or Mn were sintered at 1450 °C, and those containing Cr were sintered at 1500 °C. All materials were sintered in air as opposed to previously reported processing routes involving reducing conditions (10). In reducing conditions, dopant solubility in the YSZ lattice is likely to decrease, since the dopant would tend to reduce to metal during sintering. The material structures were examined by x-ray diffraction (XRD), while microstructures were studied by scanning electron microscopy equipped with an energy dispersive spectrophotometer (SEM/EDS). This latter technique is able to detect small amounts of second phases, usually below the resolution of XRD.

Porous platinum electrodes were deposited onto samples for electrical measurements. Impedance spectroscopy data in air were obtained from 300-800 °C in the frequency range 20-10^6 Hz. High temperature (800-1100 °C) ac conductivity measurements (at 10 kHz) were performed as a function of oxygen partial pressure between 10^{-20}-10^5 Pa. Impedance spectra were also obtained at intermittent points during the oxidation-reduction cycles. Details on the experimental set-up were presented elsewhere (15).

3. RESULTS AND DISCUSSION

3.1. Microstructural Analysis

Samples were characterized by XRD and SEM/EDS to determine the phase nature of doped YSZ, and if the dopant cations were incorporated into the YSZ structure or resulted in the formation of secondary phases. XRD results for all compositions showed that zirconia based solid solutions were present in cubic form and provided no clear evidence of secondary phases. Table 1 illustrates the effect of the different dopants on the unit cell parameter, a_0. Although irregular, the presence of Fe resulted in a slight decrease in a_0, while xMnYSZ and xCrYSZ showed very little change compared to undoped YSZ. These results are in qualitative agreement with data previously reported on these systems, although differences in materials composition with respect to this work do not allow for a direct quantitative comparison (7-9). Because of the unit cell parameter dependence on composition, and on considering the ionic radius of the different dopant cations, it can be concluded that the most likely oxidation states for the different cations are Fe^{3+}, Mn^{2+} and Cr^{3+}. These oxidation states were also assumed as dominant in previous work on these systems (7-11).

TABLE I. LATTICE PARAMETER (A_0) OF YSZ AND ALL xMYSZ COMPOSITIONS INVESTIGATED, AS DETERMINED BY XRD.

		M	
	Fe	**Mn**	**Cr**
	(Å)	**(Å)**	**(Å)**
YSZ	5.151	5.151	5.151
1MYSZ	5.131	5.148	5.154
3MYSZ	5.141	5.151	5.150
5MYSZ	5.126	5.145	5.150

SEM/EDS analysis confirmed that the sintered microstructure of all material compositions was of high density, and that no open porosity existed. Representative photomicrographs are shown in Figure 1. Additionally, in contrast to XRD results, a significant amount of a Fe-rich secondary phase was found in the 5FeYSZ composition, and a lesser amount of a Mn-rich secondary phase appeared in 5MnYSZ samples. As can be seen in Figure 2, these phases are concentrated in the grain boundary regions. The existence of such second phases only observed by SEM has already been reported in the case of Fe doped YSZ. From a previous investigation on this system it was concluded that the maximum Fe concentration into YSZ was on the order of 2 %, although for fast cooled samples Fe would be kept in solid solution up to higher concentrations (9). A further reason for the presence of secondary phases in the above mentioned compositions would be inadequate mixing of the oxide powders resulting in localized areas of high Fe and Mn concentrations, but solubility limits for the dopants are believed to be more relevant in this work.

xCrYSZ compositions showed no evidence of secondary phases either by XRD or SEM/EDS. This result is coherent with the reported solubility of at least 2 mol % Cr_2O_3 in YSZ (7), but conflicts with another study which reported a solubility limit of only 0.7 mol % Cr_2O_3 in YSZ and the appearance of Cr_2O_3 in the grain boundaries (10). In the latter work, however, the authors prepared samples by hot-pressing at 1500 °C in an inert atmosphere, using graphite dies. This corresponds to rather reducing conditions, determined by the carbon/oxygen equilibrium. While sintering, in the pre-

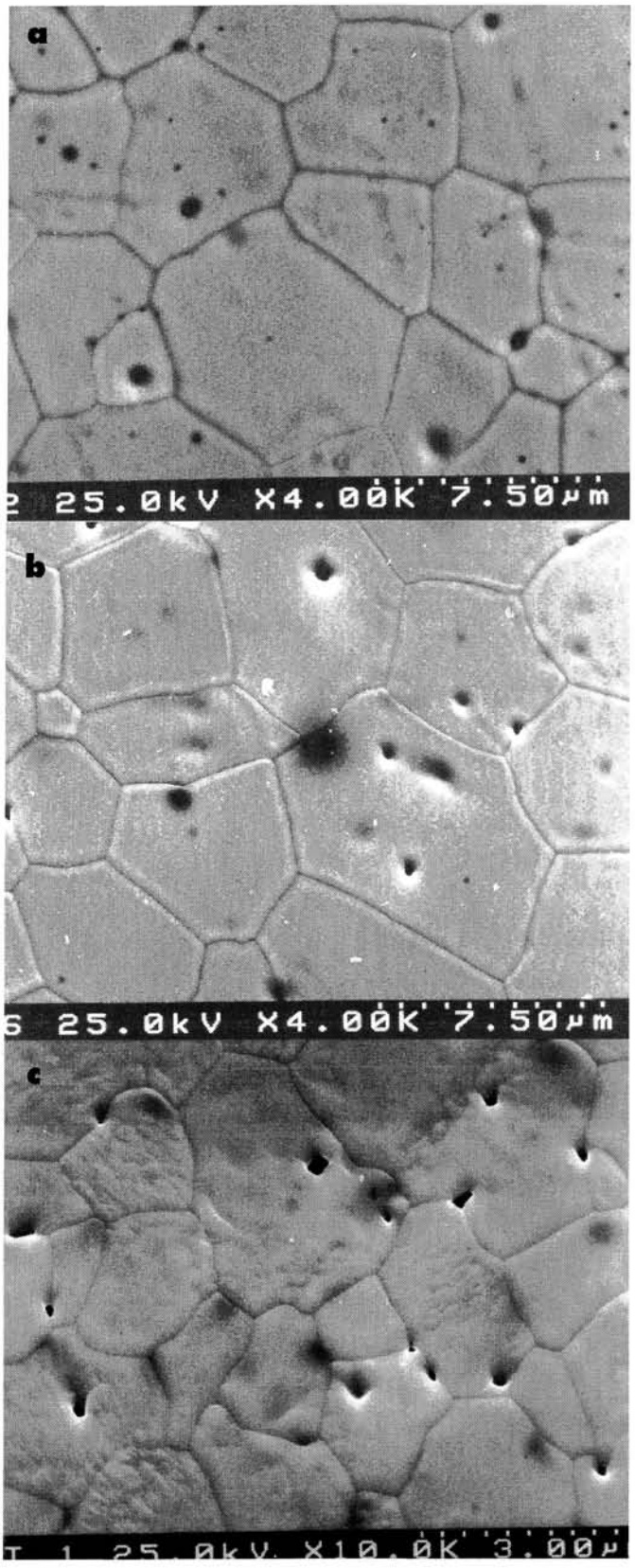

Fig. 1: *Microstructures of (a) Fe, (b) Mn and (c) Cr doped YSZ materials, after polishing and thermal etching, showing high density specimens with no open porosity.*

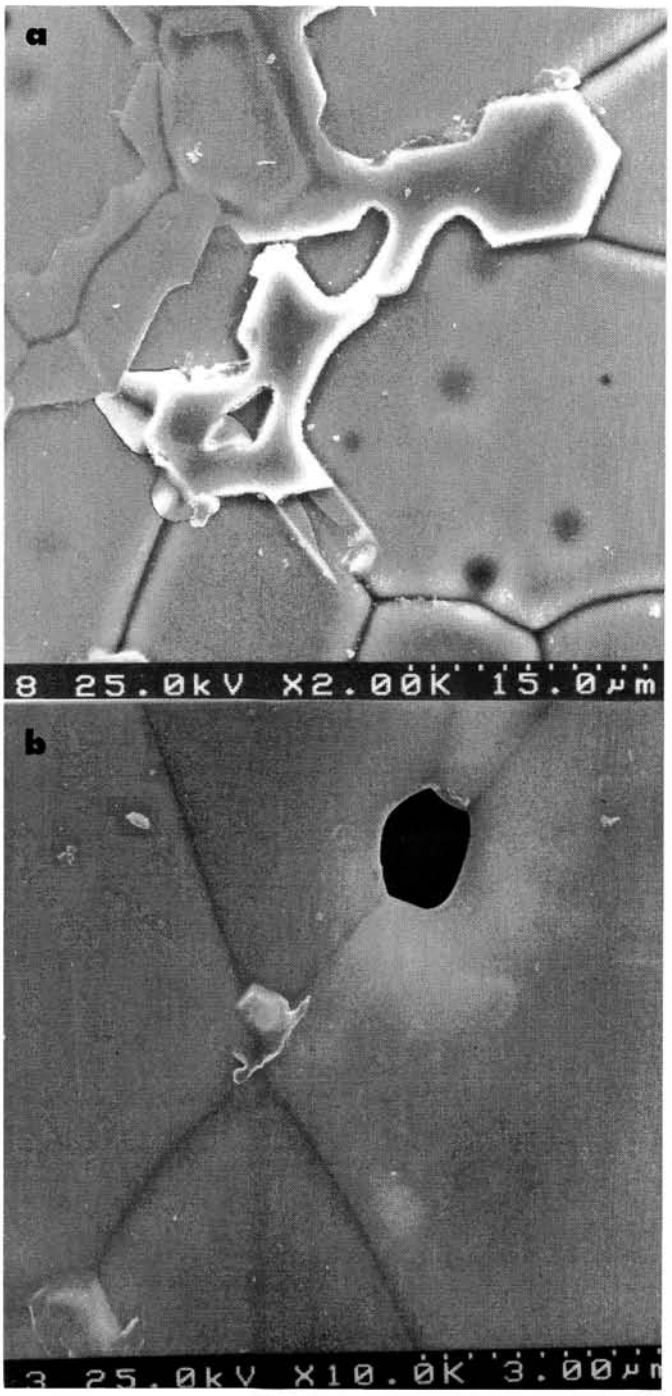

Fig. 2: *Microstructures of (a) 5FeYSZ and (b) 5MnYSZ showing the presence of secondary phases.*

sence of solid carbon, Cr_2O_3 is reduced to metallic Cr, and the solubility of the reduced metal in the YSZ lattice is minimal. After sintering, the authors annealed the samples at 1200 °C in air, in attempts to reoxidize the reduced Cr metal. However, the appearance of Cr_2O_3 in the grain boundaries of the sintered YSZ simply indicates that the insoluble metal reoxidized but could not readily diffuse through the YSZ lattice at 1200 °C.

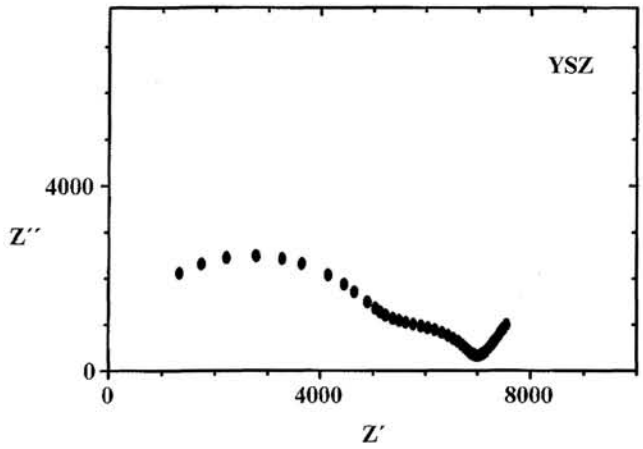

Fig. 3: *Impedance spectra of YSZ at 400 °C, in air.*

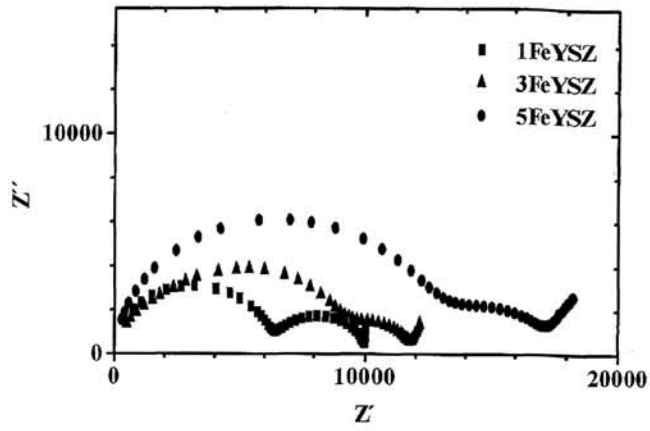

Fig. 4: *Impedance spectra of xFeYSZ at 400 °C, in air.*

3.2. Impedance Spectroscopy in Air

Impedance spectra, measured at 400 °C in air, are shown in Figures 3-6 for YSZ and all xMYSZ compositions. Data are plotted as the imaginary (Z'') versus real (Z') part of the complex impedance. As all cells had identical dimensions, analysis of their impedance spectra permits a comparison of the materials behavior. In samples containing Fe, the conductivity decreased (i.e. total Z' increased) with increasing Fe content. The conductivity of the 5FeYSZ composition was approximately 50 % of the conductivity of pure YSZ. Bulk and grain boundary impedance contributions are reasonably well separated, and the relative increase in the bulk resistance appears to be higher than that found for the grain boundary as Fe content increased. This result is coherent with previously reported data (9).

The behavior of Mn-doped compositions showed more dramatic changes. The conductivity of 5MnYSZ decreased to about 20 % of the undoped YSZ. In 1MnYSZ and 3MnYSZ, bulk and grain boundary arcs are well defined, both increasing as Mn content increased. However, the 5MnYSZ spectra exhibits one large, depressed arc aside from a possible small, low frequency contribution. Clear distinction between bulk and grain boundary contributions for this composition is, thus, inhibited.

Unlike Fe and Mn, Cr appeared to have a very small impact on the conductivity behavior of YSZ. 5CrYSZ showed a decrease in conductivity of only about 25 % in comparison to YSZ. The relative increase in the grain boundary resistance appears to be very slightly higher than the bulk resistance as Cr content increased. Overall, the impedance spectra obtained for the xCrYSZ materials most closely approximated that obtained for pure YSZ.

In Figure 7, the temperature dependence of the total conductivity is shown for YSZ and the 5MYSZ compositions, plotted in Arrhenius form. In Table 2 the calculated activation energies (E_a) are reported for the total conductivity, as well as the bulk and grain boundary conductivity of all compositions. The E_a of the grain boundary conductivity is higher than for the grains for all compositions, as usually expected. Results indicate that Cr doped compositions have the lowest activation energies and those containing Mn exhibit the higher activation energies. The overall differences, however, are quite small, suggesting that the principal defects responsible for electrical charge transport are always oxygen ion vacancies, and the defect motion mechanism is that usually established for YSZ. Note that previously published data on Mn doped YSZ suggested that the high temperature conductivity would approach YSZ, while the low temperature data would be higher than for YSZ, as a result of an activation energy much smaller than found for YSZ (7). Such findings were not verified in the present work. In addition, the effects of Cr doping on the conductivity of YSZ seen here are quite small, although previous studies showed a more noticeable decrease in conductivity (7).

In general, it could be expected that the addition of a foreign cation in YSZ would have a negative impact on the bulk conductivity, due to the different structure of the dopant oxide. A significant increase in the grain boundary resistance might also be expected if the dopant tends to segregate into the intergrain region, originating blocking grain boundaries as compared to high purity materials. However, the above results illustrate distinct differences in the behavior of doped YSZ materials, most especially when Cr is present as compared to Fe or Mn. Such differences warrant closer attention in order to understand their origins.

The role of transition metal dopants in terms of conductivity must be understood based on two important aspects:

(i) the effect of the presence of the dopants in the lattice as electrically charged defects, with the corresponding impact

TABLE II. CALCULATED ACTIVATION ENERGIES (E_A) FOR YSZ AND xMYSZ COMPOSITIONS

	Ea (total) (eV)	Ea (grain boundary) (eV)	Ea (grain) (eV)
YSZ	1.08	1.16	1.10
1FeYSZ	1.12	1.23	1.12
3FeYSZ	1.12	1.23	1.13
5FeYSZ	1.10	1.20	1.08
1MnYSZ	1.10	1.15	1.11
3MnYSZ	1.17	1.23	1.18
5MnYSZ	1.20	1.28	1.21
1CrYSZ	1.04	1.13	1.04
3CrYSZ	1.04	1.06	1.05
5CrYSZ	1.04	1.18	1.04

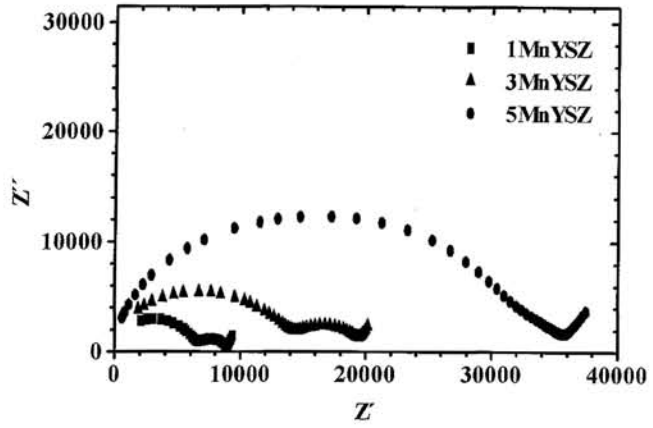

Fig. 5: *Impedance spectra of xMnYSZ at 400 °C, in air.*

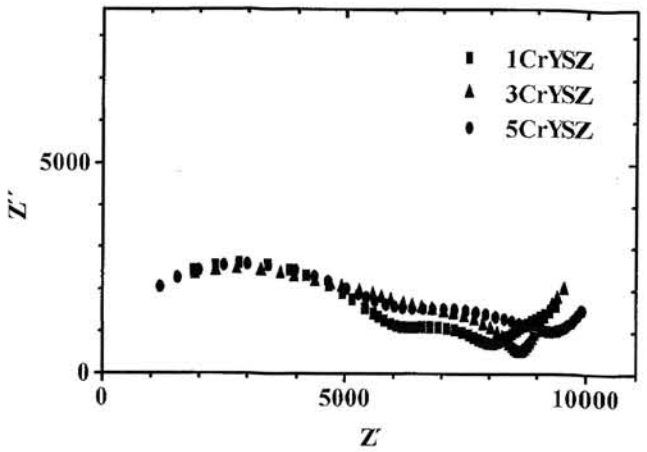

Fig. 6: *Impedance spectra of xCrYSZ at 400 °C, in air.*

of this presence on the global electroneutrality condition. This requires the identification of the position of the dopant cation in the lattice being either substitutional or interstitial, and its oxidation state.

(ii) the effect of the dopant cation in terms of lattice distortion, originated by different sizes from the host cation but also different coordination habits for the corresponding oxides.

The exact identification of the oxidation state of the cations is complex, as the stable oxidation states for all cations vary with temperature in air. However, from electrical conductivity measurements there is no evidence for any change in oxidation state. From structural characterization, as already mentioned, it can be concluded that all dopant cations have electrical charges lower than Zr^{4+}. Thus, a decrease in the total oxygen vacancy concentration determined by the presence of Y^{3+} in the lattice is not expected. The role of the dopants in terms of bulk behavior must therefore be interpreted more in terms of local structural changes. Further structural studies are in progress in attempts to answer the above questions and more precisely explain the electrical behavior of these solid solutions, however at this point, some comments can be made on this subject.

The identification of the dopant (Fe, Mn, or Cr) position in the lattice can be assumed on combining XRD with electrical conductivity data. From XRD and SEM analyses, the first impression is that the dopant cations occupy substitutional positions in the corresponding sublattice, when no secondary phases are apparent. Even when a small amount of a second phase is present, some solubility can be assumed because of the effect on lattice parameters. Furthermore, the overall electrical behavior of these materials is expected to be determined primarily by the dominant phase, at least at high temperature, and the conductivity dependence on composition further indicates that some solubility occurred.

Recent structural studies involving zirconia based materials containing dopants concluded that, depending on the dopant size, the lattice would accommodate the dopant cation with specific defect ordering processes. For dopants larger than the host cation, oxygen vacancies would mostly occupy positions near the host cation, as the Zr^{4+} ion-oxygen vacancy pairing is energetically more favorable than the equivalent pair formed with the oversized dopants. For dopants smaller than the host cation, oxygen vacancies would become associated with near neighbor undersized dopant cations (11). The dopants investigated in this work are all smaller or about the same size of Zr^{4+}. It can thus be considered that oxygen vacancies are partly trapped near dopant cations, decreasing the overall concentration of ionic defects available for electrical conduction, and resulting in a conductivity drop with increasing dopant level. Through this reasoning however, an explanation for the small effect of Cr additions as compared to the other dopants is not obvious. Further studies are required to more fully understand these materials properties.

3.3. P_{O_2} Effects on ac Conductivity

Data obtained during a redox cycle for a 5CrYSZ sample at 1000 °C are shown in Figure 8. These conductivity data should be carefully considered in terms of absolute values. As the cell resistance is quite small, compensation for the electrical connections (Pt wires) requires an accurate evaluation of the external leads contributions. The approximate compensation procedure used here resulted in some calculated cell conductivities above 10^{-1} $(\Omega\ cm)^{-1}$ a typical value of the conductivity of undoped YSZ at 1000 °C. This is contradictory to data obtained via impedance spectroscopy at lower temperatures, which indicated that the doped YSZ materials exhibited conductivities lower than undoped YSZ. Nevertheless, the qualitative dependence of conductivity on oxygen partial pressure should always be considered meaningful, although the validity of these measurements will be further discussed in the following paragraphs. Also note that consecutive redox cycles were performed beginning at 800 °C, and continuing at 100 °C intervals to a maximum temperature of 1100 °C. After a full oxidation-reduction cycle was performed, in several instances the final measured conductivity was different than the initial conductivity, which is possibly the result of segregation of the transition metal dopants at the grain boundaries.

In Figure 8, the solid symbols were estimated from conductivity measurements at 10 kHz. The 5CrYSZ sample apparently showed a drop in conductivity immediately after atmospheric reduction began, recovering under extremely reducing conditions. Similar behavior for this material was observed at lower temperatures. p-type conductivity is suggested seeing that the conductivity minimum was reached at

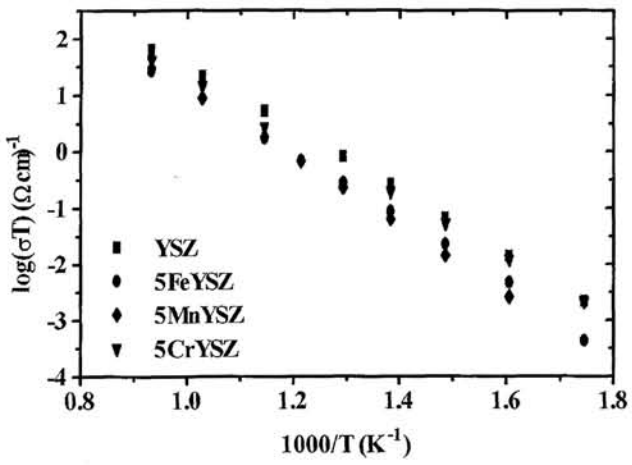

Fig. 7: *Arrhenius plot of the electrical conductivity of 5MYSZ samples, in air.*

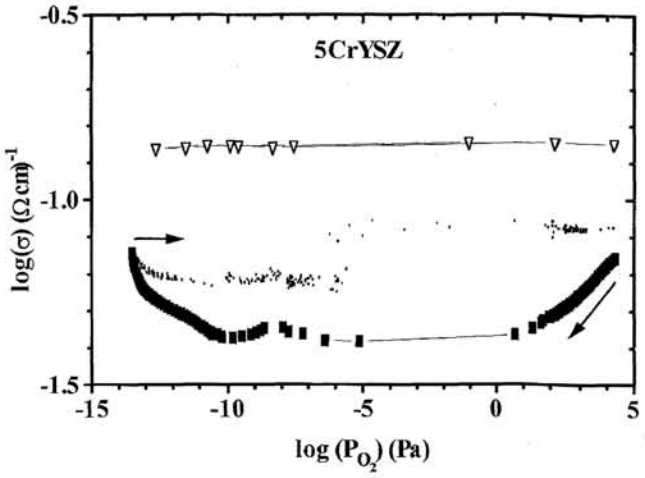

Fig. 8: *Total conductivity (at 10 kHz) as a function of oxygen partial pressure (P_{O2}) for 5CrYSZ, at 1000 °C. Solid symbols show the full redox cycle. Open symbols were estimated from impedance spectra.*

oxygen partial pressures on the order of 1 Pa. The increase in conductivity at low oxygen partial pressures suggested n-type behavior. However, conductivity data in air observed for the xCrYSZ materials (refer to Figure 7), would tend to indicate that in such conditions mixed conduction is unlikely, as it usually should be accompanied by an enhancement of the activation energy (E_a).

Figure 9 illustrates a typical impedance spectra for a YSZ based material. Three arcs exist, representing the grain, grain boundary, and electrode response to an ac signal of constant amplitude but variable frequency. The data acquisition program utilized in these studies of ac conductivity versus oxygen partial pressure measures the complex impedance, Z*, of the sample. A value of the resistance, R_{calc}, is then calculated according to the equation:

$$R_{calc} = |Z^*| . \cos\theta$$

where θ, the angle between Z* and the real axis gives a measure of the relative ratio between Z´ and Z´´. The measurement frequency must be chosen such that it well represents the overall material response of the sample (R_{TOT} in Figure 9) and θ is small (< 10 °). In this manner, errors which may result in R_{calc} are small, on the order of 1-2 %. If the measurement frequency is such that θ is too large, errors in R_{calc} become more significant and will not provide an accurate measure of R_{TOT}. Instead, the actual material resistance will be overestimated or underestimated, depending upon where the response of the material lies at the measured frequency. Referring to Figure 9, frequencies applied near point *a* will result in an underestimation of R_{TOT}, and the conductivity will appear to be higher than it truly is. Applied frequencies near point *b* will result in an overestimation of R_{TOT}, and a lower apparent conductivity.

To check for the consistency of the previous ac conductivity measurements performed at a constant frequency of 10 kHz, impedance spectroscopy data were collected at intermittent points during the oxidation-reduction cycle to more accurately determine how R_{TOT} changed as a function of oxygen partial pressure. A typical example of such measurements is shown in Figure 10 for 5CrYSZ. The open symbols seen in Figure 8 illustrate the total material conductivities as determined from these impedance spectra. It can be seen that the conductivity remained essentially constant throughout the oxygen partial pressure range scanned, and the curves taken at 10 kHz are not accurate representations of the overall material behavior. Previously, it had been verified that high temperature measurements at this frequency were representative of the overall material behavior for zirconia based systems, as well as other ionic or mixed conductors with the perovskite or pyrochlore structure (16,17). However, the presence of the transition metal dopants resulted in a shift of this frequency response into the electrode arc. Additionally, the location of the 10 kHz frequency shifted during the oxidation-reduction cycle, and θ values varied from as small as -5 ° to as large as -40 °, depending upon the temperature, oxygen partial pressure and the transition metal present. Therefore, the conductivities measured from this technique were lower than the actual overall material conductivities, and the effective electrical conductivity estimated from full impedance spectra appears to be independent of oxygen partial pressure. No electronic conductivity can, therefore, be assumed for the range of working conditions exploited in this work. The same trends were observed with the remaining 5MYSZ compositions.

4. CONCLUSIONS

Differences in the conductivity of YSZ doped with small amounts of transition metal oxides have been noted as compared to undoped YSZ materials. Differences exist as a function of the type and amount of dopant present, and the major trend is a decrease in conductivity with increasing dopant content. Based upon preliminary measurements of high temperature electrical conductivity at different oxygen partial pressures, electronic conductivity does not appear to be greatly enhanced by the presence of up to 5 % Fe, Mn, or Cr. Further investigations are necessary to better evaluate how transition metal dopants affect the electrical properties of YSZ.

ACKNOWLEDGEMENTS

Financial support is gratefully acknowledged from the Luso-American Educational Commission through a U.S. Fulbright Full Grant for R.M. Slilaty. ◆

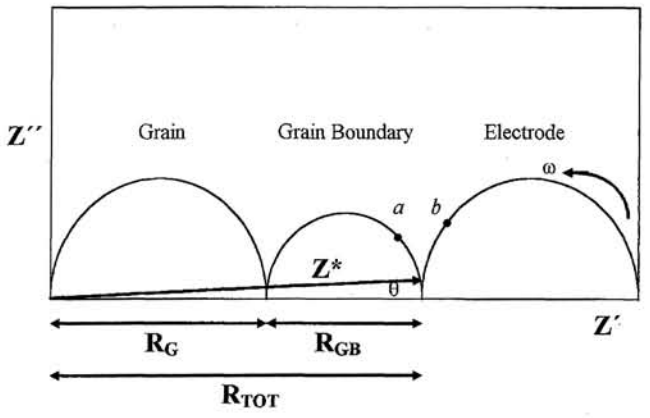

Fig. 9: *Schematic representation of a typical impedance spectra of a solid electrolyte, showing the correlation between the full impedance, Z*, at a given frequency and the overall material resistance, R_{TOT}. ac conductivity measurements made at frequencies near point a will underestimate R_{TOT}, and those made at frequencies near point b will overestimate R_{TOT}.*

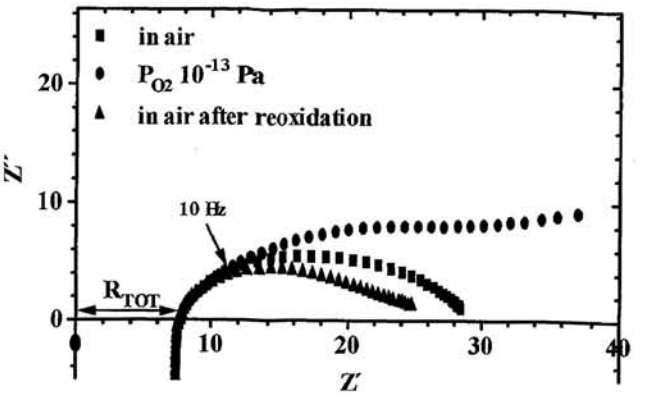

Fig. 10: *Impedance spectra obtained in air, at a P_{O2} of 10^{-13} Pa, and after reoxidation for 5CrYSZ, showing the overall material resistance, R_{TOT}, and the location of the 10 kHz data point.*

REFERENCES

1. H.L. Tuller, in Non-stoichiometric Oxides, ed. O. Toft Sorensen, Academic Press, N.York (1981), pp. 271.
2. S.S. Liou, W.L. Worrell, Electrical Properties of Novel Mixed-Conducting Oxides, Appl. Physics A, 49, (1989) 25.
3. B. Calés, J.F. Baumard, Conduction and Defect Structure of ZrO_2-CeO_2-Y_2O_3 Solid Solutions, J. Electrochem. Soc. 131, (1983) 2407.
4. P.V. Ananthapadmanabhan, N. Venkatramani, V.K. Rohatgi, A.C. Momin, K.S. Venkateswarlu, Structure and Ionic Conductivity of Solid Solutions in the System $0.9\{(ZrO_2)_{1-x}\text{-}(CeO_2)_x\}0.1(Y_2O_3)$, J. Eur. Ceram. Soc., 6, (1990) 111.
5. R.M.C. Marques, F.M.B. Marques, J.R. Frade, Characterization of Mixed Conductors by dc Techniques. Part II: Experimental Results, Solid State Ionics, 73 (1994) 26.
6. M.T. Colomer, L.S.M. Traqueia, J.R. Jurado, F.M.B. Marques, Role of Grain Boundaries on the Electrical Properties of Titania Doped Yttria Stabilized Zirconia, Mat. Res. Bull.,30, 4 (1995) 515.
7. K.W. Browall, R.H. Doremus, Synthesis and Evaluation of Doped Y_2O_3 Stabilised ZrO_2 for the Production of Hydrogen, J. Am. Ceram. Soc., 60, 5-6 (1977) 262.
8. R.V. Wilhelm, Jr., D.S. Howarth, Iron Oxide Doped Yttria-Stabilized Zirconia Ceramic: Iron Solubility and Electrical Conductivity, Am. Ceram. Soc. Bull., 58, 2 (1979) 228.
9. M.J. Verkerk, A.J.A. Winnubst, A.J. Burggraaf, Effect of Impurities on Sintering and Conductivity of Yttria-Stabilized Zirconia, J. Mat. Sci., 17 (1982) 3113.
10. M. Jayaratna, M. Yoshimura, S. Somiya, Electrical Conductivity of Cr_2O_3-Doped Y_2O_3-Stabilized ZrO_2, J. Mat. Sci., 22 (1987) 2011.
11. P. Li, I-W. Chen, J.E. Penner-Hahn, Effect of Dopants on Zirconia Stabilization - An X-ray Absorption Study: I-Trivalent Dopants, J. Am Ceram. Soc., 77, 1 (1994) 118.
12. S.C. Singhal, Tubular Solid Oxide Fuel Cells, in Proc. 3rd. Int. Symp. on Solid Oxide Fuel Cells, ed. S.C. Singhal, H. Iwahara, The Electrochemical Society, Inc., Pennington (1993) p. 665.
13. E. Ivers-Tiff,e, W. Wersing, H. Greiner, Ceramic Components for Solid Oxide Fuel Cells (SOFC) with Metallic Interconnector, in Electroceramics IV, vol. II, ed. R. Waser, S. Hoffmann, D. Bonnenberg, Ch. Hoffmann, Augustinus Buchhandlung, Aachen (1994) p.719.
14. P. Bohac, A. Orliukas, L.J. Gauckler, Lowering of the Cathode Overpotential of SOFC by Electrolyte Doping, ref.(13), p.771.
15. F.M.B. Marques, G.P. Wirtz, Electrical Properties of Ceria-Doped Yttria, J. Am. Ceram. Soc., 74 (1991) 598.
16. J.A. Labrincha, F.M.B. Marques, J.R. Frade, $La_2Zr_2O_7$ Formed at Ceramic Electrode/YSZ Contacts, J. Mat. Sci. 28 (1993) 3809.
17. J.A. Labrincha, J.R. Frade, F.M.B. Marques, Defect Structure of $SrZrO_3$, Solid State Ionics 61 (1993) 71.

Recibido: 22-6-95.
Aceptado: 15-2-96.

Trabajo presentado en la II Reunión Nacional de Electrocerámica.

BOLETIN DE LA SOCIEDAD ESPAÑOLA DE Cerámica y Vidrio

Nueva Junta Directiva de la Sociedad Española de Cerámica y Vidrio

La Sociedad Española de Cerámica y Vidrio ha procedido a la renovación estatutaria de su Junta Directiva tras las elecciones celebradas el pasado día 26 de abril de 1996.

De acuerdo con los resultados la nueva Junta Directiva queda constituida de la siguiente manera:

PRESIDENTE:	**MIGUEL ANGEL DELGADO MENDEZ** (MINCER ASOCIADOS)
VICEPRESIDENTES:	**RAFAEL DE RAMON GARCIA** (CRISTALERIA ESPAÑOLA, S.A.) **JORGE BAKALI BAKALI** (ESMALTES, SA)
SECRETARIO GENERAL:	**EMILIO CRIADO HERRERO** (INSTITUTO DE CERAMICA Y VIDRIO)
	VICESECRETARIO-GERENTE: FRANCISCO CAPEL DEL AGUILA (INSTITUTO DE CERAMICA Y VIDRIO)

■ SECCION DE ARTE Y DISEÑO

PRESIDENTE:	MARGARITA BECERRIL ROCA (ESC.MADRILEÑA DE CERAMICA DE LA MONCLOA)
VICEPRESIDENTE:	MARIBEL GARCIA VARGAS (ESC.MADRILEÑA DE CERAMICA DE LA MONCLOA)
SECRETARIO:	JAIME COLL CONESA (MUSEO NACIONAL DE CERAMICA «GONZALEZ MARTI»)

■ SECCION DE CERAMICA BLANCA Y REVESTIMIENTOS CERAMICOS

PRESIDENTE:	Mª DOLORES LLANES (ROCERSA)
VICEPRESIDENTE:	PURIFICACION ESCRIBANO (UNIVERSIDAD JAUME I DE CASTELLON)
SECRETARIO:	FRANCISCO CORMA CANOS (QPT CONSULTING)

■ SECCION DE CIENCIA BASICA

PRESIDENTE:	ANGEL CABALLERO CUESTA (INSTITUTO DE CERAMICA Y VIDRIO)
VICEPRESIDENTE:	JOSE EMILIO ENRIQUE NAVARRO (UNIVERSIDAD JAUME I, AICE)
SECRETARIO:	JOSE FRANCISCO FERNANDEZ LOZANO (INSTITUTO DE CERAMICA Y VIDRIO)

■ SECCION DE ESMALTES SOBRE METAL

PRESIDENTE:	ADOLFO CAMPOY GARCIA (FERRO ENAMEL ESPAÑOLA)
VICEPRESIDENTE:	GUILLERMO MONROS TOMAS (UNIVERSIDAD JAUME I DE CASTELLON)
SECRETARIO:	JUAN CARDA CASTELLO (UNIVERSIDAD JAUME I DE CASTELLON)

■ SECCION DE LADRILLOS Y TEJAS

PRESIDENTE:	FERNANDO PALAU CASEÑE (PALAU-CERAMICA DE CHILOECHES)
VICEPRESIDENTE:	LEOPOLDO ARCHE PEREZ-VENERO (CERAMICAS COVADONGA)
SECRETARIO:	FRANCISCO MORALES POYATO (INSTITUTO DE CERAMICA Y VIDRIO)

■ SECCION DE MATERIAS PRIMAS

PRESIDENTE:	VICENTE VARONA FERNANDEZ (G.M.A.)
VICEPRESIDENTE:	ANGEL CACERES JIMENEZ (MINCER ASOCIADOS)
SECRETARIO:	FLORA BARBA MARTIN-SONSECA (INSTITUTO DE CERAMICA Y VIDRIO)

■ SECCION DE REFRACTARIOS

PRESIDENTE:	JUAN JOSE PEREZ GALLEGO (NORTON IBERICA, C.I.,SA)
VICEPRESIDENTE:	HUMBERTO LOMBA SANCHEZ (JOSE A. LOMBA CAMIÑA)
SECRETARIO:	CARMEN BAUDIN DE LA LASTRA (INSTITUTO DE CERAMICA Y VIDRIO)

■ SECCION DE VIDRIOS

PRESIDENTE:	JOSE ANTONIO COTOS (CRISTALERIA ESPAÑOLA, S.A.)
VICEPRESIDENTE:	JUAN MANUEL MARTIN CANO (ANFEVI)
SECRETARIO:	ALICIA AMPARO DURAN CARRERA (INSTITUTO DE CERAMICA Y VIDRIO)

Desde estas páginas queremos expresar nuestro agradecimiento a todas aquellas personas que han cesado en sus cargos así como desear los mayores éxitos a los que asumen por primera vez responsabilidades en el seno de la Sociedad.

La nueva Directiva tomará posesión de sus cargos con ocasión del XXXVI CONGRESO NACIONAL DE CERAMICA Y VIDRIO a celebrar los próximos días 10, 11 y 12 de junio de 1996 en San Sebastián.